Int. J. Electrochem. Sci., 17 **(2022)** Article Number: 221188, doi: 10.20964/2022.11.78

International Journal of
ELECTROCHEMICAL
SCIENCE
www.electrochemsci.org

A highly sensitive electrochemiluminescence sensor based on antimony tin oxide/TiO_2 for detection of gastrin-releasing peptide (ProGRP)

Qinghong Wu and Wenjuan Zheng[*]

Department of Emergency, The Second People's Hospital of Lishui, Lishui 323000, Zhejiang Province, China
[*]E-mail: lswqh667091@163.com

Received: 1 September 2022 / *Accepted:* 8 October 2022 / *Published:* 20 October 2022

Progastrin-releasing peptide (ProGRP) is a highly reliable, specific and sensitive tumor marker for small cell lung cancer, thus the measurement of ProGRP levels can realize the diagnosis, prediction of prognosis and treatment monitoring of small cell lung cancer. Aptamer can bind specifically to proteins or other substances with high selectivity and affinity, and it has more stable chemical properties than antibodies. In this work, an electrochemiluminescent aptamer sensor was constructed for ProGRP detection based on AgNPs composites. For the sensor, luminol was used as the luminol, hydrogen peroxide was used as the co-reaction reagent, and titanium dioxide and AgNPs were used to enhance the luminescence, which improved the luminescence intensity and sensitivity of the sensor. The linear detection range was 10 fg/mL-12 ng/mL with a detection limit of 1.3 fg/mL under optimal experimental conditions.

Keywords: Aptasensor; Electrochemical luminescence; ProGRP; Ag nanoparticle; Nano antimony tin oxide

1. INTRODUCTION

In 1978, McDonald et al.[1] isolated a gastrin-releasing peptide (GRP), a gastrointestinal hormone with a pro-gastrin secretory effect, from pig stomach tissue. GRP is composed of 27 amino acids and is a potent pro-secretory and regulatory peptide that is widely found in the gastrointestinal tract, pulmonary respiratory tract and nervous system of mammals[2,3]. GRP is present in high levels in fetal and neonatal bronchial epithelial endocrine cells, while it is present only in neural tissue of adults and in a small proportion of neuroendocrine cells of the lung at low levels[4]. It was found that lung cancer cells themselves can produce and secrete GRP to regulate the growth of the cancer cells in an autocrine manner, and in the meantime it can also bind to receptors on the membranes of surrounding

tumor cells in a locally diffuse manner to stimulate the growth of tumor [5]. GRP is regarded as an autonomous growth factor in small cell lung cancer (SCLC), and low levels of GRP can stimulate DNA synthesis in SCLC cells. Maruno et al.[6] demonstrated for the first time that GRP is an important product of SCLC, and is also an important tumor marker for SCLC. GRP secreted by many SCLC cell lines or tumor tissues is stored in the Golgi apparatus in the cytoplasm[7]. Research show that under appropriate conditions, GRP is released into the tissues and binds to GRP receptors on the cell membrane, which supports the growth of cancer cells and their unlimited proliferation. However, the unstable active part of GRP in blood makes it susceptible to rapid degradation caused by peptide chain endolyases[8]. Therefore, the difficulty in extracting reliable GRP directly from plasma increases, thus it is more challenging to apply GRP at clinical level. ProGRP is a precursor structure of GRP, a product encoded by the GRP gene and a tumor marker for SCLC, which is commonly found in non-gastric sinus tissue, nerve fibers, neuroendocrine cells of brain and lung[9,10]. ProGRP can be divided into three molecular isoforms based on the variation of some of its amino acids, which share a common carbon terminal sequence (31-98). GRP is obtained from the hydrolytic cleavage of ProGRP, whose hydrolysis occurs in the lys-lys portion of the polypeptide sequence at positions 29-30[11], followed by the release of the carbon-terminal sequence. One of the amino acid regions, 43-97, is a conserved region and can only be found in mammals. A large number of studies have confirmed that ProGRP levels are representative of GRP levels and GRP gene expression, being a new highly reliable, sensitive and specific tumor marker [12,13].

Currently, the commonly used methods for measuring ProGRP are mainly based on immunological principles, such as enzyme-linked immunoblotting (ELISA), radioimmunoassay (RIA), chemiluminescence immunoassay (CLIA), and time-resolved immunofluorescence assay (TRIFMA)[14–17]. Among these methods, ELISA is the most commonly applied, due to its good specificity and high sensitivity. However, it requires batch testing and is not able to provide timely reports to meet clinical needs[18,19]. Monoclonal antibodies to isotope iodine-131-labeled gastrin-releasing peptide precursors are ideal for radioimmunoassay and radioimmunotherapy, but RIAs are subject to radioactive contamination. CLIA and TRIFMA are new methods that have been developed in recent years with high speed, high sensitivity and good specificity, and they can easily be automated[20].

Nucleic acid aptamers have gained extensive attention since their appearance due to their precise recognition, easy synthesis and easy modification in vitro[21–23]. In terms of basic research, the mechanism of binding nucleic acid aptamers to the corresponding ligands is the focus. In addition, studies in the mechanism of gene expression regulation and proteomics have also been emphasized. In terms of applied research, aptamers have a positive prospect for application in a number of fields such as disease detection, drug development, clinical treatment, analytical chemistry, etc. In particular, with the combination of aptamer technology and nanomaterials, certain results have been achieved in the application of biosensors, new drug development and some other fields[24]. Electrochemiluminescence (ECL) is a chemiluminescence phenomenon in which a luminous body undergoes a high-energy electron conversion reaction at the surface of an electrode by an applied voltage to produce luminescence. ECL has unique advantages in photoluminescence, bioluminescence and chemiluminescence. First, ECL does not require an external light source, which simplifies the detection device and also reduces the background noise of conventional photoluminescent sensing systems[25,26]. Second, compared with

CL, for ECL, it is easy to control the timing and location of the luminescence reaction, for the reason that it occurs only in the diffusion layer of the electrode. ECL has higher selectivity and reproducibility than CL, since it allows a better control of the light emission position. Moreover, based on this advantage, multiple targets can be measured simultaneously in the same sample with multiple electrodes[27]. Third, ECL is usually a non-destructive system, because the luminophores in the ECL can be regenerated after electrochemiluminescence emission, which allows the luminophores to participate again in the ECL reaction in excess of the co-reactants[28]. As a result, many photons are generated in each measurement cycle, thus greatly increasing the sensitivity of the technique.

Currently, luminol, bipyridine pegs, quantum dots and nanometallic clusters are used for ECL. Most researchers have used nanomaterials to prepare the sensor in order to improve the luminescence performance of luminol, and the more commonly used nanomaterials include AuNPs, AgNPs, TiO_2, Fe_3O_4, etc. TiO_2 is a typical semiconductor material with good biocompatibility, large specific surface area, and low cost, compared with other nanomaterials, which facilitates the mass production of sensors at a later stage[29]. Silver nanoparticles (AgNPs) are outstanding nanocatalytic materials that have demonstrated strong catalytic effect on luminescence and they can immobilize aptamers containing hydrophobic groups on the electrode surface via Ag-S bonds[30]. Considering the above factors, an electrochemiluminescent aptamer sensor for ProGRP detection was constructed with TiO_2 and AgNPs materials in this work. On the one hand, TiO_2 was adopted to improve the luminescence of the sensor and increase its electrochemical luminescence intensity. On the other hand, the superior catalytic effect of AgNPs was used to further improve this luminescence effect, aiming to obtain electrochemiluminescent sensors with better sensitivity. This work also investigated the electrochemical and electrochemiluminescent behavior of the above nanomaterials on the electrode surface and further explored the detection performance of the ECL aptamer sensor for ProGRP.

2. EXPERIMENTAL

2.1. Regents

Antimony tin oxide (ATO, particle size: 27nm; specific surface area:≥75 m^2/g; resistivity:≤20 Ω/cm) nanoparticles, titanium dioxide (40 nm) were purchased from Beijing Deco Island Gold Technology Co. Chitosan, anhydrous and ethanol were purchased from Sinopharm Chemical Reagent Co. Luminol was purchased from J&K Scientific Ltd. Bovine serum albumin was purchased from Shanghai Biotech Biological Co. Potassium ferricyanide and potassium ferricyanide were purchased from Tianjin Yongda Chemical Reagent Co. Hydrogen peroxide was purchased from Laiyang Economic and Technological Development Zone Fine Chemical Factory. Trisodium citrate was purchased from Tianjin Bodi Chemical Co. The aptamer sequences applied in this work were 5'-CATGCGGAGTAGATTCGAGCCCAGATAGTCCCTGGTTATTTCCTTAGG-3', which is synthesized by Shanghai Sangong Biotechnology Co.

2.2. Preparation of luminol, ATO/TiO_2 and AgNPs

2 g of NaOH was dissolved in 500 mL of ultrapure water to obtain a 0.1 M solution of sodium hydroxide. Afterwards, 0.8 g of luminol was added to 30 mL of the above prepared NaOH solution. In the following step, the mixture was stirred and an appropriate amount of ultrapure water was added to completely dissolve the luminol. Finally, the obtained luminol solution was added to 500 mL of ultrapure water to obtain a final 0.01 M luminol solution.

0.05 g of CS was dissolved in 100 mL of 1.0% acetic acid solution and stirred for 3 h at room temperature to dissolve CS completely to prepare 0.05% chitosan solution. 3 mg of ATO powder and 3.75 mg of TiO_2 powder were dissolved in 10 mL of 0.05% chitosan solution. The above mixture should be sonicated in an ultrasonic cleaner (40 KHz, 150 W) for 2~3 h. After that, the solution was shaken in a rotary shaker for 4 h until it reached a homogeneous and stable state.

25 mL of 1 mM silver nitrate solution was added dropwise to 75 mL of 2 mM sodium borohydride solution with vigorous stirring that lasted for 10 min, after which 5 mL of 1% mass fraction sodium citrate solution was added to the above solution with vigorous stirring to stabilize the AgNPs.

2.3. Preparation of electrochemiluminescence sensor

The electrochemiluminescent aptamer sensor was assembled with the following steps: 1 μL of ATO@TiO_2 material was added dropwise to the glassy carbon electrode (GCE) and dried at RT to obtain ATO-TiO_2/GCE. 1 μL of luminol solution was added dropwise to the electrode and dried at room temperature to obtain luminol/ATO-TiO_2/GCE. After that, 2 μL of AgNPs was coated to obtain AgNPs/luminol/ATO-TiO_2/GCE. 2 μL of ProGRP aptamer was then added dropwise to the electrode surface, and the aptamer was immobilized on the electrode surface by silver-sulfur bonding. Finally, Apt/AgNPs/luminol/ATO-TiO_2/GCE was immersed in BSA solution to seal the non-specific sites, and the sensor was assembled, as shown in Figure 1. Sensors without applying luminol during fabrication were named as AgNPs/ATO-TiO_2/GCE and Apt/AgNPs/ATO-TiO_2/GCE.

To test the effectiveness of the sensor in detection, the prepared sensor was immersed in ProGRP and incubated for 30 min, and the unattached ProGRP was rinsed off with ultrapure water. The luminescence cell was filled with an appropriate amount of 10 nM hydrogen peroxide solution (pH=8), and the luminescence detection was performed with the electrochemiluminescence system. The detection principle of this sensor platform is that after binding to ProGRP, a ProGRP aptamer complex was formed, affecting the luminol luminescence, thus the luminescence intensity was reduced.

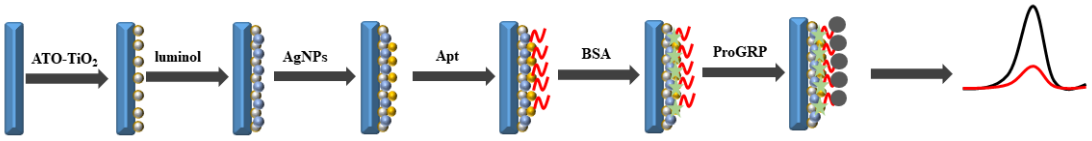

Figure 1. Schematic diagram of aptasensor assembled procedure.

3. RESULTS AND DISCUSSION

In order to verify the performance of nanomaterials such as ATO, the modification process was first characterized by CV and DPV (Figure 2). Both DPV and CV experiments were performed in test solutions containing 5 mM $[Fe(CN)_6]^{3-/4-}$ and 0.1 M KCl. Figure 2A shows that the redox peaks of the bare electrode are small. As ATO-TiO_2 is immobilized, the electrochemical resdox of ATO-TiO_2/GCE increases, showing a pair of large redox peaks. When the GCE surface is modified with AgNPs, the peak current decreases, which means that the electrical conductivity decreases[31,32]. The peak current decreases significantly after the immobilization of aptamer and BSA[33]. The experimental results of DPV characterization are similar to CV characterization, as shown in Figure 2B. The aptamer is modified to the electrode surface by covalent bonding, and the Apt/AgNPs/ATO-TiO_2/GCE current signal further decreases, for the reason that the aptamer itself is non-conductive and hinders the electron transfer[34].

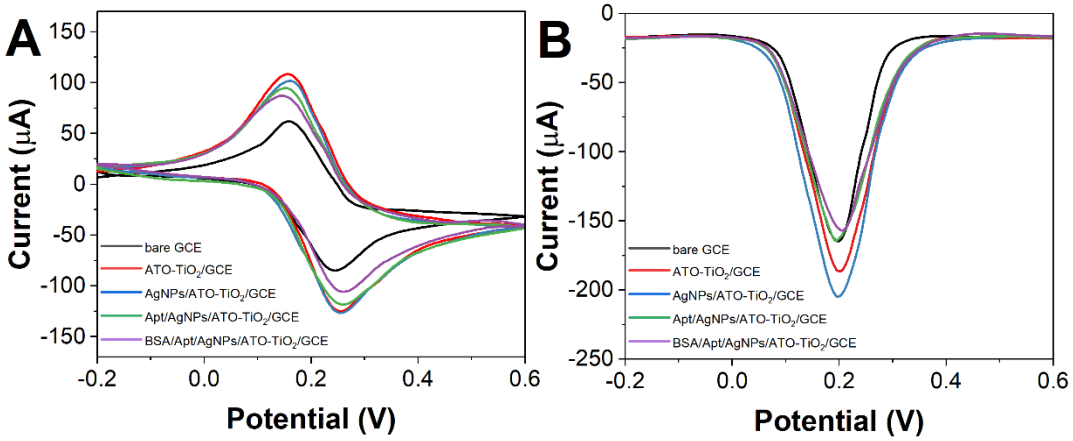

Figure 2. (A) CVs and (B) DPVs of bare GCE, ATO-TiO_2/GCE, AgNPs/ATO-TiO_2/GCE, Apt/AgNPs/ATO-TiO_2/GCE and BSA/Apt/AgNPs/ATO-TiO_2/GCE in 5 mM $[Fe(CN)_6]^{3-/4-}$ + 0.1 M KCl.

Figure 3 presents the ECL of the sensor at different assembly steps. When the electrode is not modified with any nanomaterial, the GCE has a small luminescence peak in the presence of luminol. As the electrode is modified with ATO-TiO_2 composite nanomaterials, the luminescence intensity of the electrode increases by more than two times, indicating that the ATO-TiO_2 composite nanomaterials have excellent electrochemiluminescence properties[35]. The luminescence intensity is further enhanced after the modification with AgNPs, indicating a good catalytic effect of AgNPs on the electrochemiluminescence reaction. Despite that the luminescence of the sensor is enhanced by modifying only ATO-TiO_2 or AgNPs nanomaterials, it is much smaller than the luminescence of the two materials in combination. The modification with ProGRP aptamer hinders the free electron transfer in the sensor, resulting in a decrease in luminescence intensity[36]. When the electrode is modified with bovine serum albumin, the luminescence intensity is further reduced, since it is a large molecule protein with a strong inhibitory effect on the whole luminescence process.

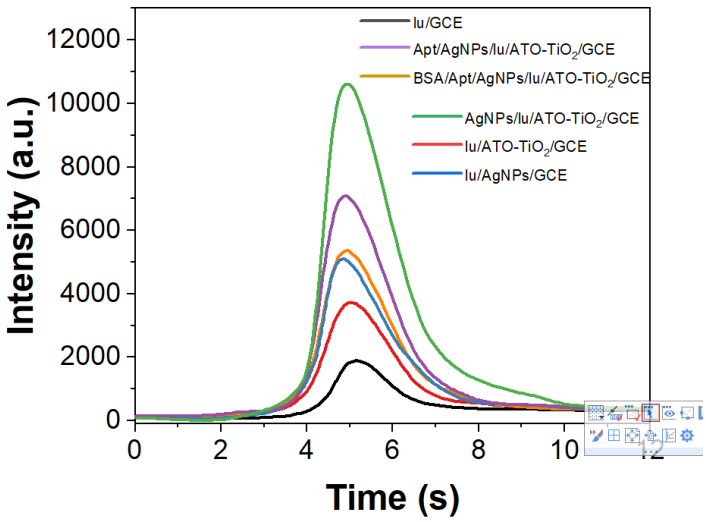

Figure 3. ECLs of luminol/GCE, luminol/ATO-TiO_2/GCE, luminol/AgNPs/GCE, AgNPs/luminol/ATO-TiO_2/GCE, Apt/AgNPs/luminol/ATO-TiO_2/GCE and BSA/Apt/AgNPs/luminol/ATO-TiO_2/GCE.

The aptamer concentration has a large effect on the electrochemiluminescence sensor, thus this work optimized this condition, with the experimental results shown in Figure 4A. A low intensity of luminescence shows with a low aptamer concentration. The luminescence intensity rises with the aptamer concentration. When the aptamer exceeds 100 nM, the luminescence signal decreases rather than increases. Therefore, 100 nM was chosen as the optimal concentration for the construction of the aptamer sensor.

The pH of the reaction system environment has a large impact on the electrochemical sensor. The performance of the sensor is affected in excessive acidity or alkalinity, for the binding affinity of the aptamer and ProGRP is reduced in such environments. In addition, the luminescence of luminol is also influenced by the pH of the reaction cell. The luminescence intensity is higher under weakly alkaline conditions[37], while the luminescence is not obvious under neutral or acidic environmental conditions. Therefore, in this work, different pH of PBS were used to prepare the H_2O_2 reaction substrate to control the pH of the whole sensor, and the experimental results are shown in Figure 4B. It can be seen that the luminescence of the sensor increases rapidly at pH=7.0 to 9.0. When pH>9.0, the luminous intensity of the sensor rapidly decreases. Therefore, 9.0 was chosen as the optimal pH for the sensor.

In order to achieve excellent sensor performance, experiments were conducted to optimize the incubation time of ProGRP with aptamers. The incubation time mainly affects the number of ProGRP binding to the aptamer on the electrode, which in turn affects the luminescence performance of the whole sensor. Figure 4C reveals that the electrochemiluminescence intensity gradually increases with the incubation time, and finally remains stable after 30 min. However, the ProGRP aptamer complex formed on the sensor surface reaches the saturation value as reaching a time threshold, and the electrochemiluminescence intensity value does not change significantly even if the incubation time increases [38]. Therefore, 30 min was chosen as the optimal incubation time for the aptamer and ProGRP.

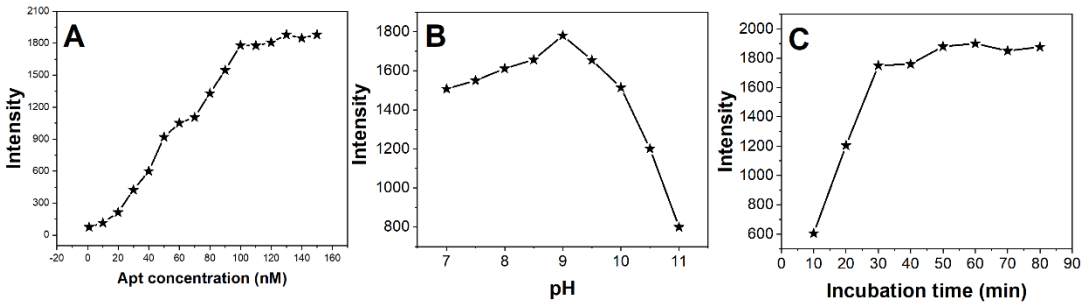

Figure 4. Optimization of experiment conditions: (A) aptamer concentration, (B) pH, (C) incubation time.

Under the optimal experimental conditions, the prepared electrochemiluminescent aptamer sensors were immersed in different concentrations of ProGRP, thus the aptamer and ProGRP were fully bound, and then electrochemiluminescence tests were performed in 10 nM hydrogen peroxide solution[39]. Figure 5A demonstrates the DPV responses of BSA/Apt/AgNPs/luminol/ATO-TiO_2/GCE towards ProGRP detection. The experimental results show that the logarithm of ProGRP has a linear relationship with the electrochemiluminescence intensity. The minimum detection limit of the calculation was 1.3 fg/mL. Table 1 shows the results of the comparison between this sensor and other methods used to detect ProGRP. It can be found that this sensor has a very promising application with a low detection limit and a wide detection range.

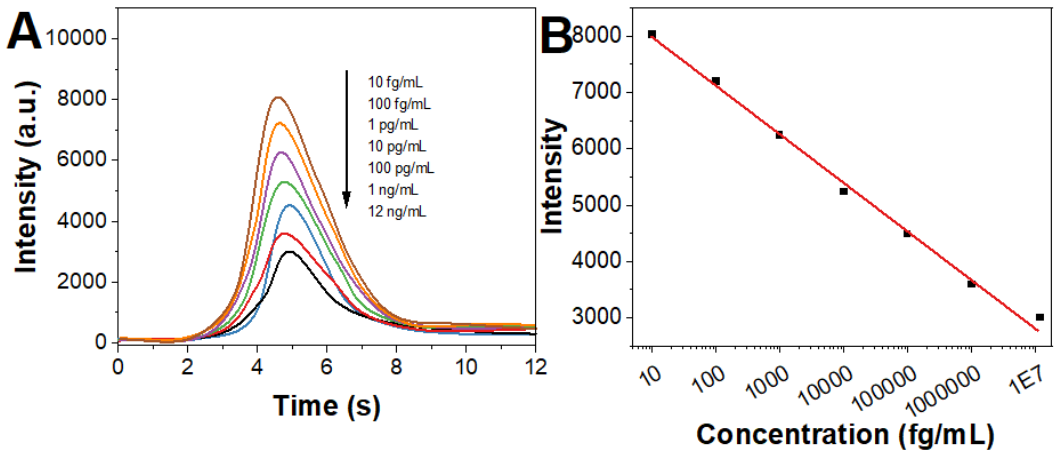

Figure 5. (A) DPV responses and (B) calibration curves of BSA/Apt/AgNPs/luminol/ATO-TiO_2/GCE towards ProGRP detection.

Good specificity is one of the advantages of the aptamer sensor and one of the performance indicators for which this sensor needs to be tested. Three substances that often exert effects were selected for the detection of interfering terms of ProGRP. The experimental results are shown in Figure 6. The interfering substances include 100 pg/mL carcinoembryonic antigen (CEA), squamous cell carcinoma

antigen (SCCA), human epididymis protein 4 (HE4), interleukin-6 (IL-6) and ProGRP. According to the results, the luminescence of the sensor is significantly reduced only in the presence of ProGRP, indicating that the presence of other substances does not interfere with the detection of ProGRP and that the sensor has good selectivity. Moreover, a standard addition recovery test was performed to investigate the ProGRP detection in human serum samples to explore the reliability of the constructed sensor. Different concentrations of ProGRP (50 pg/mL, 100 pg/mL) were added into 10-fold diluted serum. As shown in Table 2, the recoveries are estimated to be 103.9–107.8%, with RSD of 1.6–2.1%. As a result, the detection performance of the ECL sensor is satisfactory.

Table 1. Sensing performance of the proposed BSA/Apt/AgNPs/luminol/ATO-TiO_2/GCE with previous reports.

Sensor	Linear range (fg/mL)	LOD (fg/mL)	Ref.
AuNP/2D-MoS_2/GCE	20 pg/mL-5 ng/mL	3.2 pg/mL	[11]
MWNTs modified GCE	50-1000 pg/mL	10 pg/mL	[40]
Au/TiO_2	10-500 pg/mL	3 pg/mL	[41]
3D-rGO@Au	1 fg/mL-10 ng/mL	0.14 fg/mL	[42]
BSA/Apt/AgNPs/luminol/ATO-TiO_2/GCE	10 fg/mL-12 ng/mL	1.3 fg/mL	This work

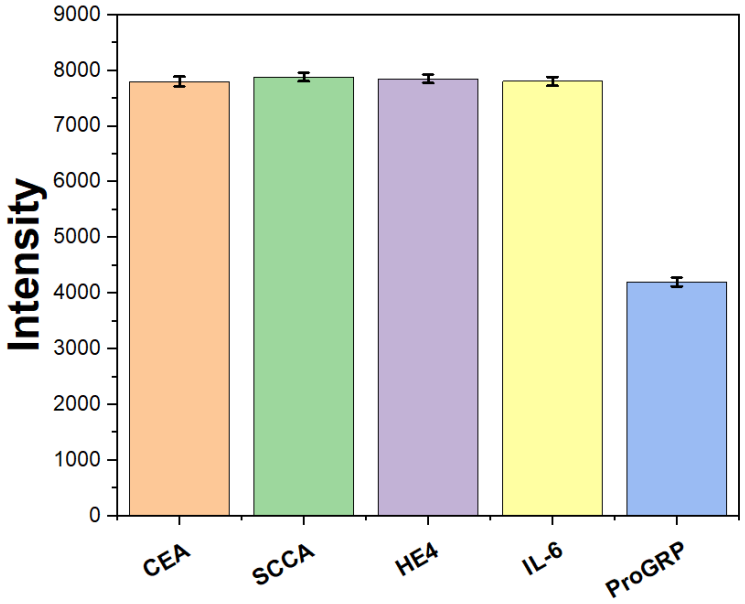

Figure 6. Intensity of BSA/Apt/AgNPs/luminol/ATO-TiO_2/GCE towards 100 pg/mL of CEA, SCCA, HE4, IL-6 and ProGRP.

Table 2. The spike recovery test for ProGRP detection in serum sample.

Samples	Found (pg/mL)	Added (pg/mL)	Found (pg/mL)	Recovery (%)	RSD (%, n=3)
Human serum	27.2	50	80.2	103.9	2.1
	27.5	100	137.5	107.8	1.6

4. CONCLUSION

In this paper, a ProGRP ECL aptamer sensor based on ATO-TiO_2 and AgNPs is proposed. The experiment results show that TiO_2 can greatly improve the luminescence performance of the biosensor due to its good photoelectric properties. In addition, AgNPs can play the catalytic role to further enhance the luminescence of the sensor. AgNPs also stabilize the aptamer on the electrode surface through silver-sulfur bonding to achieve accurate and sensitive detection of ProGRP. Under optimal experimental conditions, the linear equation of the logarithm of its concentration versus luminescence intensity was obtained. The linear detection range for ProGRP was 10 fg/mL to 12 ng/mL and the minimum detection limit of the sensor was calculated to be 1.3 fg/mL. The research results provide a practical method for the rapid detection of ProGRP in medical clinical applications.

References

1. T. McDonald, G. Nilsson, M. Vagne, M. Ghatei, S. Bloom, V. Mutt, *Gut*, 19 (1978) 767–774.
2. L. Baratto, H. Jadvar, A. Iagaru, *Mol. Imaging Biol.*, 20 (2018) 501–509.
3. L. Baratto, R. Laudicella, M. Picchio, S. Baldari, A. Iagaru, *Clin. Transl. Imaging*, 7 (2019) 39–44.
4. Z. Dai, J. Zhu, H. Huang, L. Fang, Y. Lin, S. Huang, F. Xie, N. Sheng, X. Liang, *Nephrology*, 25 (2020) 398–405.
5. L. Guo, X. Wu, Y. Zhang, F. Wang, J. Li, J. Zhu, *Hepatol. Res.*, 49 (2019) 247–255.
6. K. Maruno, K. Yamaguchi, K. Abe, M. Suzuki, N. Saijo, Y. Mishima, N. Yanaihara, Y. Shimosato, *Cancer Res.*, 49 (1989) 629–632.
7. P. Hoppenz, S. Els-Heindl, M. Kellert, R. Kuhnert, S. Saretz, H.-G. Lerchen, J. Köbberling, B. Riedl, E. Hey-Hawkins, A.G. Beck-Sickinger, *J. Org. Chem.*, 85 (2020) 1446–1457.
8. X. Liu, X. Liu, J. Cai, Z. Xun, Q. Song, R. Wang, G. Li, Z. Xu, *BioMed Res. Int.*, 2022 (2022) 1775190.
9. K. Michalski, L. Kemna, J. Asberger, A.L. Grosu, P.T. Meyer, J. Ruf, T. Sprave, *Cancers*, 13 (2021) 6106.
10. Y. Tu, J. Tao, F. Wang, P. Liu, Z. Han, Z. Li, Y. Ma, Y. Gu, *Biomater. Sci.*, 8 (2020) 2682–2693.
11. X. Wang, H. Deng, C. Wang, Q. Wei, Y. Wang, X. Xiong, C. Li, W. Li, *Analyst*, 145 (2020) 1302–1309.
12. J.W. Wiggins, J.E. Sledd, L.M. Coolen, *Front. Neurol.*, 12 (2021) 982.
13. L.-J. Zhi, A.-L. Sun, *Anal. Chim. Acta*, 1134 (2020) 106–114.
14. M. Bohler, C. Dougherty, T. Tachibana, E.R. Gilbert, M.A. Cline, *Neurosci. Lett.*, 713 (2019) 134529.
15. A. Ghosh, K. Woolum, S. Kothandaraman, M.F. Tweedle, K. Kumar, *Molecules*, 24 (2019) 2878.
16. A. Hirooka, M. Hamada, D. Fujiyama, K. Takanami, Y. Kobayashi, T. Oti, Y. Katayama, T.

Sakamoto, H. Sakamoto, *Sci. Rep.*, 11 (2021) 13315.
17. P. Hoppenz, S. Els-Heindl, A.G. Beck-Sickinger, *J. Pept. Sci.*, 25 (2019) e3224.
18. O. Kayalar, F. Oztay, H.G. Ongen, *Cell Commun. Signal.*, 18 (2020) 96.
19. J. Kurth, B.J. Krause, S.M. Schwarzenböck, C. Bergner, O.W. Hakenberg, M. Heuschkel, *Eur. J. Nucl. Med. Mol. Imaging*, 47 (2020) 123–135.
20. J. Lau, E. Rousseau, Z. Zhang, C.F. Uribe, H.-T. Kuo, J. Zeisler, C. Zhang, D. Kwon, K.-S. Lin, F. Bénard, *ACS Omega*, 4 (2019) 1470–1478.
21. R. Li, R. Gao, Y. Wang, Z. Liu, H. Xu, A. Duan, F. Zhang, L. Ma, *Sci. Rep.*, 10 (2020) 11434.
22. C. Liolios, B. Buchmuller, U. Bauder-Wüst, M. Schäfer, K. Leotta, U. Haberkorn, M. Eder, K. Kopka, *J. Med. Chem.*, 61 (2018) 2062–2074.
23. E. Lymperis, A. Kaloudi, W. Sallegger, I.L. Bakker, E.P. Krenning, M. de Jong, T. Maina, B.A. Nock, *Bioconjug. Chem.*, 29 (2018) 1774–1784.
24. C. Morgat, R. Schollhammer, G. Macgrogan, N. Barthe, V. Vélasco, D. Vimont, A.-L. Cazeau, P. Fernandez, E. Hindié, *PloS One*, 14 (2019) e0210905.
25. B.A. Nock, D. Charalambidis, W. Sallegger, B. Waser, R. Mansi, G.P. Nicolas, E. Ketani, A. Nikolopoulou, M. Fani, J.-C. Reubi, T. Maina, *J. Med. Chem.*, 61 (2018) 3138–3150.
26. T. Oti, R. Ueda, R. Kumagai, J. Nagafuchi, T. Ito, T. Sakamoto, Y. Kondo, H. Sakamoto, *Int. J. Mol. Sci.*, 22 (2021) 10362.
27. A. Pagoto, F. Garello, G.M. Marini, M. Tripepi, F. Arena, P. Bardini, R. Stefania, S. Lanzardo, G. Valbusa, F. Porpiglia, M. Manfredi, S. Aime, E. Terreno, *Mol. Imaging Biol.*, 22 (2020) 85–93.
28. H.-J. Park, Y. Kim, M.-K. Kim, J.J. Hwang, H.J. Kim, S.-K. Bae, M.-K. Bae, *Cells*, 9 (2020) 737.
29. K. Takanami, T. Oti, Y. Kobayashi, K. Hasegawa, T. Ito, N. Tsutsui, Y. Ueda, E. Carstens, T. Sakamoto, H. Sakamoto, *J. Comp. Neurol.*, n/a (2022).
30. X.-F. Wang, B.-H. Zhang, X.-Q. Lu, R.-Q. Wang, *J. Cell. Physiol.*, 234 (2019) 1567–1577.
31. J. Guo, S. Li, J. Wang, J. Wang, *Sens. Actuators B Chem.*, 346 (2021) 130548.
32. S. Hou, P. Wang, Y. Nie, Y. Guo, Q. Ma, *Chem. Eng. J.*, 446 (2022) 136906.
33. L. Hu, M. Lei, J. Zhang, Y. Dong, *Sens. Actuators B Chem.*, 344 (2021) 130328.
34. S. Li, X. Ma, C. Pang, M. Wang, G. Yin, Z. Xu, J. Li, J. Luo, *Biosens. Bioelectron.*, 176 (2021) 112944.
35. G. Mo, X. He, C. Zhou, D. Ya, J. Feng, C. Yu, B. Deng, *Biosens. Bioelectron.*, 126 (2019) 558–564.
36. P. Rebelo, J.G. Pacheco, I.V. Voroshylova, M.N.D.S. Cordeiro, C. Delerue-Matos, *Electrochimica Acta*, 397 (2021) 139273.
37. X. Shan, Y. Pan, F. Dai, X. Chen, W. Wang, Z. Chen, *Microchem. J.*, 155 (2020) 104708.
38. L. Shang, X. Wang, W. Zhang, L.-P. Jia, R.-N. Ma, W.-L. Jia, H.-S. Wang, *Sens. Actuators B Chem.*, 325 (2020) 128776.
39. D. Wang, S. Jiang, Y. Liang, X. Wang, X. Zhuang, C. Tian, F. Luan, L. Chen, *Talanta*, 236 (2022) 122835.
40. Z. Zhong, N. Peng, Y. Qing, J. Shan, M. Li, W. Guan, N. Dai, X. Gu, D. Wang, *Electrochimica Acta*, 56 (2011) 5624–5629.
41. Y. Zhuo, Y.-Q. Chai, R. Yuan, L. Mao, Y.-L. Yuan, J. Han, *Biosens. Bioelectron.*, 26 (2011) 3838–3844.
42. Y. Liu, S. Si, S. Dong, B. Ji, H. Li, S. Liu, *Microchem. J.*, 170 (2021) 106644.